

Strain dependence of transition temperatures and structural symmetry of BiFeO₃ within the tetragonal-like structure

W. Siemons, G. J. MacDougall, A. A. Aczel, J. L. Zarestky, M. D. Biegalski et al.

Citation: *Appl. Phys. Lett.* **101**, 212901 (2012); doi: 10.1063/1.4767335

View online: <http://dx.doi.org/10.1063/1.4767335>

View Table of Contents: <http://apl.aip.org/resource/1/APPLAB/v101/i21>

Published by the [American Institute of Physics](http://www.aip.org).

Related Articles

Enhanced ferromagnetism and glassy state in phase separated La_{0.95}Sr_{0.05}MnO_{3+δ}

J. Appl. Phys. **112**, 103907 (2012)

Hard ferromagnetism in melt-spun Hf₂Co₁₁B alloys

Appl. Phys. Lett. **101**, 202401 (2012)

Magnetic field driven transition from an antiferromagnetic ground state to a ferrimagnetic state in Rb_{0.19}Ba_{0.3}Mn_{1.1}[Fe(CN)₆]·0.48H₂O Prussian blue analogue

J. Appl. Phys. **112**, 093903 (2012)

Superior magnetic softness at elevated temperature of Si-rich Fe-based nanocrystalline alloy

J. Appl. Phys. **112**, 083922 (2012)

Reversible solid-state hydrogen-pump driven by magnetostructural transformation in the prototype system La(Fe,Si)₁₃Hy

J. Appl. Phys. **112**, 083918 (2012)

Additional information on *Appl. Phys. Lett.*

Journal Homepage: <http://apl.aip.org/>

Journal Information: http://apl.aip.org/about/about_the_journal

Top downloads: http://apl.aip.org/features/most_downloaded

Information for Authors: <http://apl.aip.org/authors>

ADVERTISEMENT

AIP | Applied Physics
Letters

SURFACES AND INTERFACES
Focusing on physical, chemical, biological, structural, optical, magnetic and electrical properties of surfaces and interfaces, and more...

ENERGY CONVERSION AND STORAGE
Focusing on all aspects of static and dynamic energy conversion, energy storage, photovoltaics, solar fuels, batteries, capacitors, thermoelectrics, and more...

EXPLORE WHAT'S NEW IN APL

SUBMIT YOUR PAPER NOW!

Strain dependence of transition temperatures and structural symmetry of BiFeO₃ within the tetragonal-like structure

W. Siemons,¹ G. J. MacDougall,² A. A. Aczel,² J. L. Zarestky,^{3,4} M. D. Biegalski,⁵ S. Liang,^{1,6} E. Dagotto,^{1,6} S. E. Nagler,^{2,7} and H. M. Christen¹

¹Materials Science and Technology Division, Oak Ridge National Laboratory, Oak Ridge, Tennessee 37831, USA

²Quantum Condensed Matter Division, Oak Ridge National Laboratory, Oak Ridge, Tennessee 37831, USA

³Department of Physics and Astronomy, Iowa State University, Ames, Iowa 50011, USA

⁴Division of Materials Science and Engineering, Ames Laboratory, Iowa State University, Ames, Iowa 50011, USA

⁵Center for Nanophase Materials Science, Oak Ridge National Laboratory, Oak Ridge, Tennessee 37831, USA

⁶Department of Physics and Astronomy, University of Tennessee, Knoxville, Tennessee 37996, USA

⁷CIRE, University of Tennessee, Knoxville, Tennessee 37996, USA

(Received 19 September 2012; accepted 30 October 2012; published online 21 November 2012)

The influence of strain-imposed in-plane lattice symmetry on the structural and magnetic properties of tetragonal-like BiFeO₃ is investigated by x-ray and elastic neutron scattering. We find that an increase in the in-plane distortion results in an increase of the Néel temperature from 313 ± 5 K to 324 ± 3 K for films grown on YAlO₃ and LaAlO₃, respectively. The change in magnetic ordering temperature is reproduced in three-dimensional Heisenberg Monte-Carlo simulations. These results show that strain cannot be treated as a single scalar number or simply as a direct consequence of the lattice mismatch between the film material and the substrate. © 2012 American Institute of Physics. [<http://dx.doi.org/10.1063/1.4767335>]

Bismuth ferrite (BiFeO₃, BFO) is the only known material with robust multiferroicity above room temperature and is of great scientific interest for that reason.¹ In bulk form, BFO has a rhombohedral crystal structure with the ferroelectric polarization pointing along the pseudocubic $\langle 111 \rangle_{pc}$ directions (the subscript *pc* will be used to denote pseudocubic indices) and G-type antiferromagnetic ordering. Although the bulk properties are interesting, most of the research on BFO has been performed on thin films, in particular, because the ferroelectric properties are superior in thin films compared to most bulk samples due to reduced leakage, and because epitaxial films are more readily obtained than single crystals. The most important reason for studies on epitaxial films, however, is that such samples make it possible to apply biaxial stress, and thus, to study the influence of lattice symmetry on the material's properties.

Stress imposes a strain (σ , relative to the bulk rhombohedral unit cell) on the material through epitaxial constraint to the chosen substrate due to the mismatch σ_{fs} between the substrate's pseudocubic lattice parameter $a_{pc,s}$ and the bulk lattice parameter of the film, $a_{pc,f}^{bulk}$: $\sigma_{fs} = (a_{pc,s} - a_{pc,f}^{bulk})/a_{pc,f}^{bulk}$. Note that this mismatch between bulk BiFeO₃ and the substrate is not necessarily equal to the actual film's lattice distortion $\sigma = (a_{pc,f} - a_{pc,f}^{bulk})/a_{pc,f}^{bulk}$ except if the film is coherently strained, i.e., with an in-plane lattice parameter that is exactly equal to that of the substrate, $a_{pc,f} = a_{pc,s}$. For relatively small amounts of mismatch, for example, by growing on SrTiO₃ with lattice parameter $a = 3.905$ Å (compared to BFO $a_{pc,f}^{bulk} = 3.97$ Å, $\sigma_{fs} \approx -1.6\%$), the crystal structure of BFO is described as monoclinic, but closely resembles the bulk rhombohedral structure. For this reason, this phase is described as R-like BFO. When matching to a substrate yields a compressive strain that exceeds $\sigma \approx -4.5\%$ the out-of-plane lattice parameter increases by over 20% and the

unit cell, although still monoclinic,^{2,3} resembles a highly strained tetragonal one (T-like).⁴⁻⁶ Recent theoretical predictions⁷ additionally indicate a strong effect of biaxial compression (assuming perfect film/substrate coherence) within this T-like structure on spin order. Application of such large amounts of stress is accomplished by growth on LaAlO₃ ($a_{pc} = 3.79$ Å, $\sigma_{fs} \approx -4.5\%$) or YAlO₃ ($a_{pc} = 3.69$ Å, $\sigma_{fs} \approx -7.0\%$). As our experiments presented below show, the description of strain as a scalar number fails in the case of BiFeO₃ on LaAlO₃ and YAlO₃—and the strain along each of the two monoclinic axes needs to be considered independently. Furthermore, coherence between the film and substrate lattice is not observed in either case.

The magnetic and ferroelectric properties are strongly influenced by strain and have been extensively studied experimentally for R-like BFO.⁸⁻¹⁰ For T-like BFO, such experimental observations are still lacking and in this letter, we focus on the influence of strain through applied stress on the magnetic properties of T-like BFO grown on LaAlO₃ (LAO) and YAlO₃ (YAO).

Films were grown using pulsed laser deposition (PLD) with a 248 nm KrF excimer laser from a 10% excess Bi target at 2 Hz. During deposition, the substrate was kept at 650 °C in 25 mTorr oxygen background pressure, resulting in a deposition rate of approximately 0.05 Å/pulse. The total thickness of the films is 125 nm for the film on YAO and 300 nm for that on LAO.

X-ray diffraction was performed on a PANalytical X'Pert thin film diffractometer using Cu K α radiation equipped with an Anton-Paar hot stage where needed. Out-of-plane and in-plane $\theta/2\theta$ measurements at room temperature (see Figs. 1(a) and 1(b), respectively) show that the majority phase in both films is T-like BFO. The film on LAO has an additional temperature dependent phase which arises

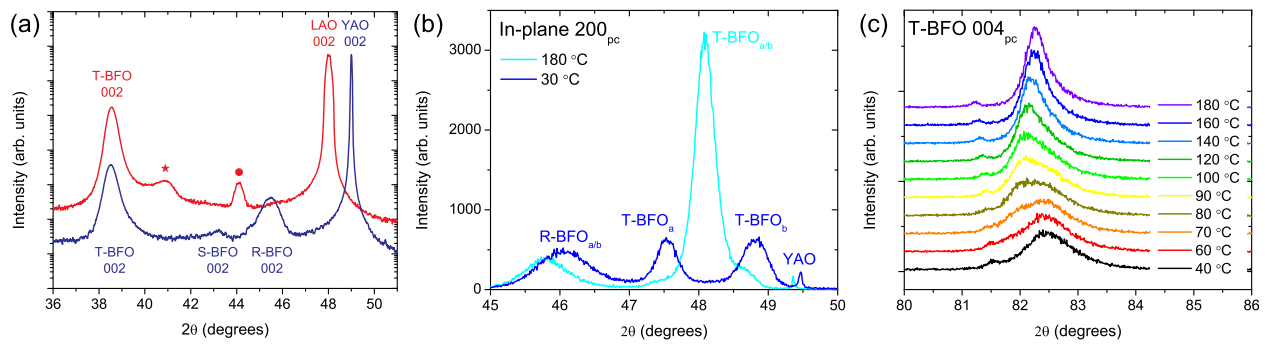


FIG. 1. (a) X-ray diffraction pattern around the 002_{pc} peaks of T-like BFO on LAO and YAO. The peak marked with a star is a temperature dependent phase which arises reversibly below the structural phase transition temperature as discussed in the previous work;³ the peak marked with a dot is associated with the high-temperature sample stage. Other polymorphs of BFO show up in the sample grown on YAO and are labeled R- and S-BFO. (b) In-plane x-ray diffraction around the pseudocubic (200) peaks of the film on YAO. (c) Temperature dependence of the T-BFO (004) diffraction peak showing the structural phase transition temperature to be 353 K (80 °C). The small peak to the left of the main peak is associated with the high-temperature sample holder.

reversibly below the structural phase transition temperature as discussed in the previous work.³ The sample on YAO has a contribution of two other polymorphs of BFO, which are labeled S- and R-BFO (the term “S” is used here for the phase that previously has been labeled Tri-1 (Ref. 11) or M_I (Ref. 12) and with lattice parameters in-between of those of the R-like and T-like polymorphs). In agreement with the previous results,¹³ we will show in future publications that this S-phase forms as mechanism of strain relaxation upon cooling of the sample after growth, i.e., it cannot be avoided by a tuning of growth parameters, etc., except in very thin films, which would not yield sufficient neutron scattering intensity. However, due to the large difference in lattice parameters between the “S” and “T-like” polymorphs, our experiments are focused strictly on the “T-like” portion of the sample, for which we determine the structure and the magnetic properties. This separation is possible because the focus of this study is not to determine the origin of the lattice distortions, but their consequences on magnetic ordering. The lattice parameters extracted from these data are given in Table I and show that the strain in the material depends strongly on the substrate material. Most noticeably, the a/b ratio, which we take as the measure of strain symmetry, is reduced on YAO compared to LAO while the c lattice spacing is unchanged. A single scalar value thus clearly no longer represents the strain in the film, and we define $\sigma_a = (a_f - a_{pc,f}^{bulk})/a_{pc,f}^{bulk}$ for a and σ_b defined similarly for b (see Table I). We find

TABLE I. Lattice parameters and distortions of T-like BiFeO_3 at room temperature for films on LaAlO_3 and YAlO_3 .

Lattice parameters	On LaAlO_3^a	On YAlO_3
In-plane a (Å)	3.84(1)	3.82(1)
In-plane b (Å)	3.70(1)	3.73(1)
Out-of-plane c (Å)	4.672(2)	4.669(2)
Monoclinic angle β (°)	87.9(2)	88.5(3)
In-plane area (ab) (Å ²)	14.21(8)	14.25(7)
Distortion a/b	1.038(6)	1.024(5)
Tetragonality c/\sqrt{ab}	1.239(7)	1.237(7)
σ_a (%)	-3.27(3)	-3.78(3)
σ_b (%)	-6.80(5)	-6.05(5)

^aFrom Ref. 2.

that $|\sigma_a|$ is larger for BFO on LAO, $|\sigma_b|$ is larger for BFO on YAO. Surprisingly, the smaller substrate lattice parameter of YAO does not result in a decrease of the film’s in-plane unit cell area ab [$=14.21(8)$ Å² on LAO and $=14.25(7)$ Å² on YAO]. However, the a/b ratio becomes closer to unity [$=1.038(6)$ on LAO and $=1.024(5)$ on YAO]. Note that both samples are thus under strong in-plane compression when compared to rhombohedral BFO. However, with the material having undergone a strain-induced transformation to the “T-like” polymorph, a proper determination of “tensile” versus “compressive” would require a comparison to “bulk T-like” BFO—a material that does not exist. It is interesting to note, though, that calculations for the T-like unit cell predict an a/b ratio of 1.² Since the in-plane distortion in the material decreases (a/b closer to 1) when changing from LAO to YAO this might be an indication that BiFeO_3 on these two substrates is actually under tensile strain with respect to the energy minimum for “T-like” BFO. Note that experiments with films of varying thickness¹⁴ in fact also indicate that BFO on LAO is subject to tensile strain, whereas BFO on NdAlO_3 ($a_{pc} \approx 3.75$ Å) may be under compression. This would indicate that BFO on YAO should also be compressively strained, contrary to our a/b ratio considerations, and may point to a more subtle effect of substrate anisotropy.

In the previous work on BFO grown on LAO, we reported a structural phase transition at 100 °C (373 K) where the nature of the monoclinic distortion changes from a room temperature M_C type [$(100)_{pc}$ symmetry plane] to M_A [$(1\bar{1}0)_{pc}$ symmetry plane].^{3,15} Similar measurements are performed here for the sample on YAO, with the results shown in Figs. 1(b) and 1(c). We found that the structural phase transition from the M_C to M_A monoclinic phase occurs at a lower temperature for the film with less in-plane asymmetry (i.e., a/b distortion), namely at 80 °C.

We next turn our attention to the effect of lattice symmetry on the magnetic order, in particular, on the Néel temperature, T_N . Previously, we have shown that $T_N = 324$ K in T-like BFO on LAO is lower than the structural (M_C to M_A) transition temperature at $T = 373$ K.¹⁶ To determine the Néel temperature of the film grown on YAO, similar neutron scattering measurements were performed using the HB1a Triple-Axis Spectrometer at the High-Flux Isotope Reactor in an elastic configuration with a fixed incident energy

$E_i = 14.7$ meV, pyrolytic graphite (PG) (002) monochromator and analyzer, instrument collimations $48'-48'-40'-68'$, and higher order contamination removed by standard PG filters. The film was aligned in the (H H L) scattering plane. For measurements at temperatures ranging from 10 K to 375 K, the sample was mounted in a closed cycle refrigerator (CCR) in a can with thermal contact assured by He exchange gas. Additional measurements for the film on LAO from room temperature to 500 K were performed using a furnace. Where presented below, data from the furnace are scaled to match the data from the CCR using measurements of substrate and film Bragg peaks in the overlapping temperature regime as discussed extensively in our previous publication.¹⁶

In our earlier work,¹⁶ we determined that a competition of G-type and C-type antiferromagnetism may be present in T-like BFO films on LAO. In this letter, we will solely focus on the majority phase, G-type, which also has the higher Néel temperature of the two. Figures 2(a) and 2(b) show the $(\frac{1}{2} \frac{1}{2} \frac{1}{2})$ peak characteristic of G-type order at low (10 K) and high temperature (350 K) for both films. Also included are scans over the same range above the Néel temperature showing the absence of the peaks and confirming the peaks are caused by a cell doubling phase transition at a temperature well below the structural transition temperature implied by x-ray diffraction. Since no additional structural phase transition were observed by x-ray diffraction in this temperature range, the existence of the $(\frac{1}{2} \frac{1}{2} \frac{1}{2})$ peak is clearly attributed to G-type antiferromagnetic ordering (in agreement with our

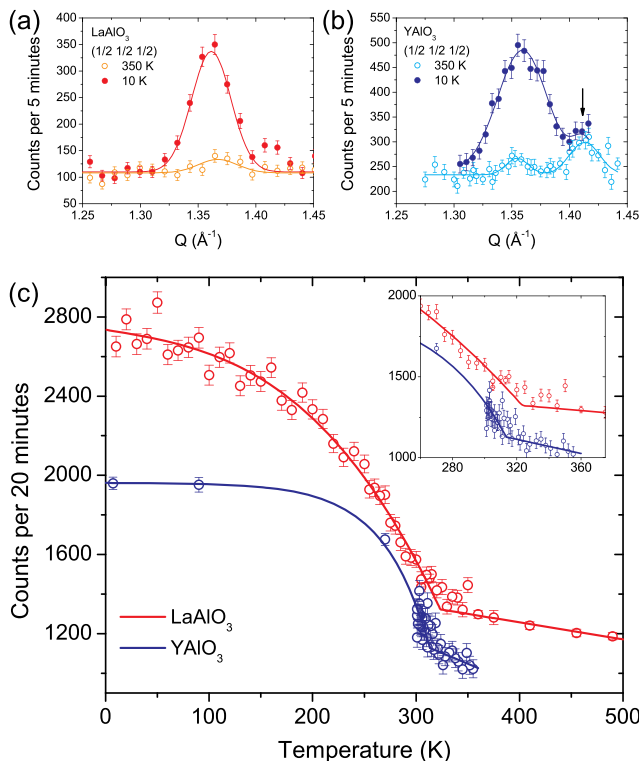


FIG. 2. Elastic neutron scattering of the T-like BFO $(\frac{1}{2} \frac{1}{2} \frac{1}{2})$ peak at 10 K and 350 K for the films grown on (a) LAO and (b) YAO. Non-magnetic contributions from the substrate are indicated with an arrow. (c) The height of the peak in (a) and (b) measured as a function of temperature. Fits were performed using a linearly sloping background and a power law function. The Néel temperature is determined by the intercept of the power law function with the sloping background.

study of BFO on LAO, where additional half-order peaks were also recorded, with their relative intensities again showing the magnetic origin of the cell doubling). Note that the measurement of the scatter intensity corresponding to a half-order peak of the T-phase selectively probes the antiferromagnetic order of this phase only: the magnetic contributions of impurity R or S phases are not characterized and do not contribute to the intensities analyzed here. By tracking the height of the peak as a function of temperature, we can determine the magnetic ordering temperature as plotted in Fig. 2(b). We find the Néel temperature to be 324 ± 3 and 313 ± 5 K for films on LAO and YAO, respectively.

In R-like BFO, the Néel temperature has a weak dependence on the amount of stress applied: Infante and coworkers⁸ found that T_N is reduced by about 8 K per percent applied (film-substrate) lattice mismatch σ_{fs} . The dependence of the Néel temperature on film-substrate lattice mismatch is graphically represented in Fig. 3, which includes the data by Infante *et al.*⁸ In order to compare the complete data set, the data need to be represented in terms of film-substrate mismatch (represented by the substrate lattice parameter) rather than actual film strain, since a scalar value no longer suffices to describe the strain, as discussed above.

The representation in Fig. 3 fails to capture the type of distortion that BFO is subject to when deposited on LAO and YAO—namely that the in-plane unit cell area ab remains constant while a/b changes. To understand the strain dependence of the Néel temperature, we begin by noting that the spin-spin coupling within the plane is dominated by nearest neighbors and falls off with Fe-Fe distance d_{Fe-Fe} as $J_{Fe-Fe} \propto (d_{Fe-Fe})^{-14}$ (this is based on Harrison's estimation for the dependence of hopping amplitudes with distance,¹⁷ as explained in Ref. 16 and references therein; our results are not sensitive to the power 14 and other power law decays lead to qualitatively similar conclusions). In the simplest model of a 2D Ising or Heisenberg spin

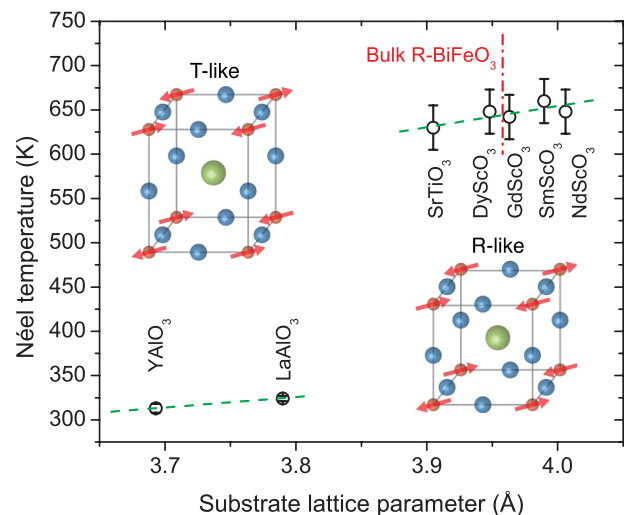


FIG. 3. The dependence of the Néel temperature of BFO on the pseudocubic lattice parameter of the substrate. In addition to the dramatic reduction in Néel temperature at the R- to T-like phase transition, a trend of decreasing Néel temperature with increased film-substrate lattice mismatch is observed both in the T-like BFO as well as in the R-like forms of BFO. The R-like BFO data were taken from Infante *et al.*⁸ The green dashed line is a linear fit through the data in the T- and R-like regions and serves as a guide to the eye.

system, one would have $T_N \propto J_a + J_b$ with in-plane coupling constants $J_a \propto a^{-14}$ and $J_b \propto b^{-14}$ (where a and b are the unit cell parameters). If the in-plane area of the unit cell remains constant, i.e., $ab = A$, it immediately follows that $J_a + J_b$ will have a minimum at $a = b$. Therefore, as the a/b ratio deviates from unity (increases), the Néel temperature will increase, just as observed in our data: In fact, as a/b increases from 1.024 to 1.038 (Table I), the term $J_a + J_b$ will increase by $\sim 4\%$, in agreement with the increase of the Néel temperature by 3.5%. However, it is clear that a mean field analysis of the anisotropic three dimensional Fe sublattice does not properly incorporate fluctuation effects that may be of relevance in our case due to the effective reduced dimensionality of the T-like BFO phase. Since in our previous work,¹⁶ we have shown that a 3D Heisenberg classical model studied with Monte Carlo (MC) simulations captures the weak but relevant component in the (longer)

c-axis direction, we have therefore carried out similar studies on the three-dimensional lattice employing a cube of side $L = 12$, sufficient to grasp the qualitative trends. Typically, 10^5 steps for thermalization and 4×10^6 equilibrium steps are performed for each temperature in order to properly incorporate the strong fluctuations that occur in these quasi-2D systems, as already indicated in our previous work.¹⁶ Figure 4(a) shows the results for T_N as a function of a/b , obtained from the specific heat measurements shown in Fig. 4(b). In these calculations, the in-plane superexchange J for the case of an undistorted system $a/b = 1$ is taken as the unit of energy. With $J_a \propto a^{-14}$ and $J_b \propto b^{-14}$, $J_a J_b = J^2$ and $J_a = (b/a)^7$ and $J_b = (a/b)^7$ were used in the MC simulations. For small values of a/b ($a/b < 1.1$), an increase in T_N is in fact observed for an increase in a/b , in good agreement with our data. Interestingly, at larger values of a/b , the reversed trend is observed. As we will show elsewhere,¹⁸ this corresponds to a transition of the system to quasi-1D spin chains, which is beyond the focus of the present effort.

To summarize, we found that for highly strained BFO the structural distortion (“strain”) within the T-like polymorph changes its symmetry (a/b distortion) but not its magnitude (in-plane lattice area ab) when the lattice mismatch between the bulk value of BFO and of the substrate is changed, indicating that a larger lattice mismatch actually results in a crystal structure closer to the one theoretically predicted. By changing the substrate from YAO to LAO (decreasing the lattice mismatch), the a/b ratio increases from 1.024 to 1.038, the structural M_C - M_A phase transition temperature increases from 353 K to 373 K, and T_N increases from 313 K to 324 K. The latter finding can be explained as a consequence of strengthened spin-spin coupling associated with the lattice distortion. These results show that unit cell distortions have a subtle effect on these phase transitions and that strain cannot be treated as a single scalar quantity.

Research supported by the U.S. Department of Energy (DOE), Basic Energy Sciences (BES), Materials Sciences and Engineering Division (H.M.C., W.S., J.L.Z., E.D., S.L.) and performed in part at the High Flux Isotope Reactor (G.J.M., A.A.A., S.E.N.) and Center for Nanophase Materials Sciences (M.D.B.), both supported at ORNL by DOE-BES.

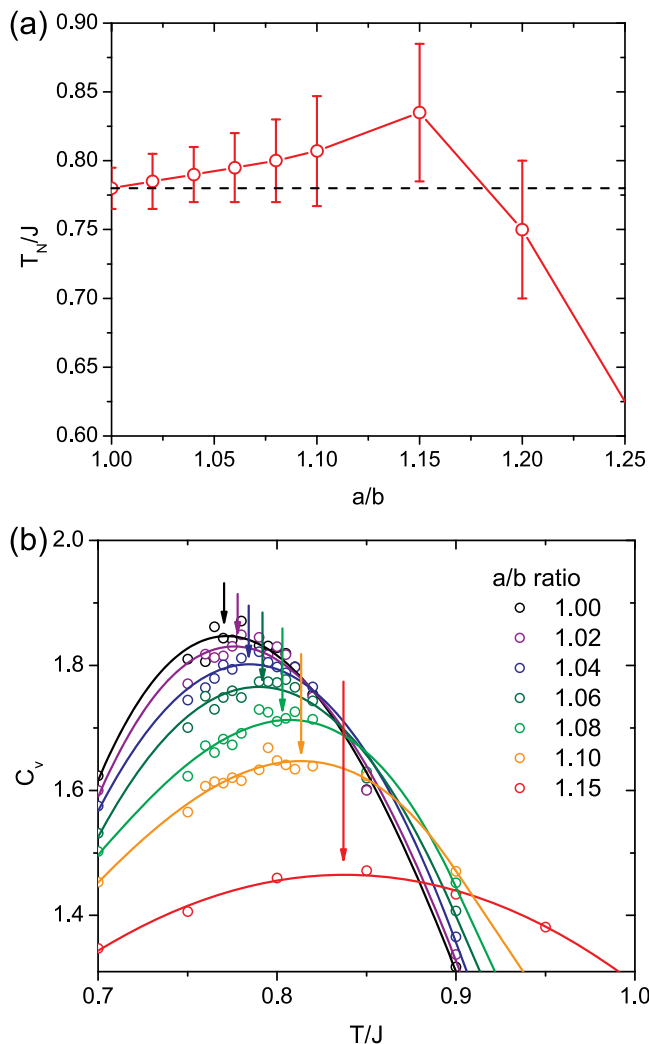


FIG. 4. (a) The Néel temperature T_N as a function of a/b , from MC simulations calculations of the 3D Heisenberg model, obtained from the specific heat measurements shown in (b), with the in-plane superexchange J for the case of an undistorted system $a/b = 1$ taken as the unit of energy. The error bars in the critical temperatures mainly reflect the size of the broad peaks found by measuring the specific heat. (b) Specific heat C_V obtained from the fluctuations of the total energy in the MC simulations vs temperature. Shown are results for several ratios a/b of interest, with the arrow indicating the location of the broad maximum for each a/b . The smooth curves are guides to the eye. The oscillations between points for a fixed a/b is a good indicator of the statistical error bars at each temperature.

¹J. Wang, J. B. Neaton, H. Zheng, V. Nagarajan, S. B. Ogale, B. Liu, D. Viehland, V. Vaithyanathan, D. G. Schlom, U. V. Waghmare, N. A. Spaldin, K. M. Rabe, M. Wuttig, and R. Ramesh, *Science* **299**, 1719 (2003).

²H. Christen, J. Nam, H. Kim, A. Hatt, and N. Spaldin, *Phys. Rev. B* **83**, 144107 (2011).

³W. Siemons, M. D. Biegalski, J. H. Nam, and H. M. Christen, *Appl. Phys. Express* **4**, 095801 (2011).

⁴H. Béa, B. Dupé, S. Fusil, R. Mattana, E. Jacquet, B. Warot-Fonrose, F. Wilhelm, A. Rogalev, S. Petit, V. Cros, A. Anane, F. Petroff, K. Bouzehouane, G. Geneste, B. Dkhil, S. Lisenkov, I. Ponomareva, L. Bellaiche, M. Bibes, and A. Barthélémy, *Phys. Rev. Lett.* **102**, 217603 (2009).

⁵D. Ricinchi, K.-Y. Yun, and M. Okuyama, *J. Phys.: Condens. Matter* **18**, L97 (2006).

⁶R. J. Zeches, M. D. Rossell, J. X. Zhang, A. J. Hatt, Q. He, C. H. Yang, A. Kumar, C. H. Wang, A. Melville, C. Adamo, G. Sheng, Y. H. Chu, J. F. Ihlefeld, R. Erni, C. Ederer, V. Gopalan, L. Q. Chen, D. G. Schlom, N. A. Spaldin, L. W. Martin, and R. Ramesh, *Science* **326**, 977 (2009).

⁷C. Escorihuela-Sayalero, O. Diéguez, and J. Íñiguez, e-print arXiv:1207.6859.

⁸I. C. Infante, S. Lisenkov, B. Dupé, M. Bibes, S. Fusil, E. Jacquet, G. Geneste, S. Petit, A. Courtial, J. Jurazsek, L. Bellaiche, A. Barthélémy, and B. Dkhil, *Phys. Rev. Lett.* **105**, 57601 (2010).

- ⁹M. D. Biegalski, D. H. Kim, S. Choudhury, L. Q. Chen, H. M. Christen, and K. Dörr, *Appl. Phys. Lett.* **98**, 142902 (2011).
- ¹⁰D. H. Kim, H. N. Lee, M. D. Biegalski, and H. M. Christen, *Appl. Phys. Lett.* **92**, 012911 (2008).
- ¹¹Z. Chen, S. Prosandeev, Z. L. Luo, W. Ren, Y. Qi, C. W. Huang, L. You, C. Gao, I. A. Kornev, T. Wu, J. Wang, P. Yang, T. Sritharan, L. Bellaiche, and L. Chen, *Phys. Rev. B* **84**, 94116 (2011).
- ¹²A. R. Damodaran, C.-W. Liang, Q. He, C.-Y. Peng, L. Chang, Y.-H. Chu, and L. W. Martin, *Adv. Mater.* **23**, 3170 (2011).
- ¹³H.-J. Liu, C.-W. Liang, W.-I. Liang, H.-J. Chen, J.-C. Yang, C.-Y. Peng, G.-F. Wang, F.-N. Chu, Y.-C. Chen, H.-Y. Lee, L. Chang, S.-J. Lin, and Y.-H. Chu, *Phys. Rev. B* **85**, 14104 (2012).
- ¹⁴C.-S. Woo, J. H. Lee, K. Chu, B.-K. Jang, Y.-B. Kim, T. Y. Koo, P. Yang, Y. Qi, Z. Chen, L. Chen, H. C. Choi, J. H. Shim, and C.-H. Yang, *Phys. Rev. B* **86**, 054417 (2012).
- ¹⁵Z. Chen, Z. Luo, C. Huang, Y. Qi, P. Yang, L. You, C. Hu, T. Wu, J. Wang, C. Gao, T. Sritharan, and L. Chen, *Adv. Funct. Mater.* **21**, 133 (2011).
- ¹⁶G. J. MacDougall, H. M. Christen, W. Siemons, M. D. Biegalski, J. L. Zarestky, S. Liang, E. Dagotto, and S. E. Nagler, *Phys. Rev. B* **85**, 100406 (2012).
- ¹⁷W. A. Harrison, *Electronic Structure and the Properties of Solids* (Dover, 1989).
- ¹⁸S. Liang and E. Dagotto “Monte Carlo study of antiferromagnetic critical temperatures in anisotropic classical three-dimensional Heisenberg models” (unpublished).